

A Priori Calculation of the Optical-Absorption Spectrum of the Hydrated Electron

Jürgen Schnitker, Kazi Motakabbir, Peter J. Rossky, and Richard Friesner

Department of Chemistry, University of Texas at Austin, Austin, Texas 78712

(Received 26 October 1987)

The optical-absorption spectrum of an excess electron solvated in a molecular sample of liquid water at 300 K has been calculated with use of solvent configurations generated via path-integral simulation and subsequent solution of the excess-electronic eigenvalue problem. Electronic transitions from an *s*-like ground state to three bound, localized, *p*-like excited states dominate the broad asymmetric spectrum with excitations into an apparent continuum following at higher energy. Asymmetric distortions and radial fluctuations of the solvent cavities contribute comparably to the spectral broadening.

PACS numbers: 71.55.Jv, 71.20.Ad, 78.40.Dw

Numerous experimental and theoretical studies have attempted to elucidate the origin of the broad and structureless optical-absorption band of solvated excess electrons in polar fluids, yet little agreement about the correct physical interpretation of the absorption process has been achieved.¹ Arguments have been advanced in favor of very different models, and fits of the observed spectra are possible on the basis of mutually exclusive assumptions.

In this Letter, we present a simulated absorption spectrum for an excess electron in liquid water at room temperature. In contrast to previous model calculations, our treatment is quantum statistical with the explicit computation of a thermal ensemble average over the solvent, with use of a large number of solvent molecules to represent the liquid. Most importantly, we invoke no adjustable parameters in the calculation. The results provide the first *a priori* description of the physics underlying the optical spectrum of the hydrated electron.

In our approach, we successively apply two computational procedures. First, we generate an ensemble of solvent configurations that is representative of the state of the hydrated electron at room temperature. This is accomplished by path-integral simulation of an excess electron immersed in a sample of 500 water molecules. In a second stage, we compute, for each of 600 solvent configurations, the excess-electronic eigenstates by explicit solution of the one-particle Schrödinger equation. Averaging over solvent configurations, we obtain the electronic excitation spectrum within the Franck-Condon approximation.

The first part of the present calculation is similar to that described in detail earlier.^{2,3} A complete report of the full technical details used here will be provided in a later paper. Here, we outline our procedure.

While the excess electron is treated as a quantum particle, the water molecules are described classically; their interactions are modeled with the well-tested simple point-charge pair potential.⁴ The interactions between excess electron and solvent molecules are described by an approximate pseudopotential described by us recently.² It accounts for static Coulomb interactions, polarization

effects, and orthogonality requirements between the excess-electronic wave function and solvent-molecular wave functions. The solvent molecules and excess electron are confined to a cubic box of side length 24.66 Å, corresponding to a density of 0.977 g cm⁻³, and the usual periodic boundary conditions are employed.

Accounting for the quantum dispersion of the excess electron by a discretized path-integral representation,⁵ we sample from the canonical ensemble of this system ($T=300$ K). We employ a path-integral discretization of $P=1500$. After equilibration, 30 000 configurations are generated by the method of constant-temperature molecular dynamics,⁶ corresponding to a classical water simulation of 60 ps. All pair interactions are evaluated with a spherical cutoff that is smoothly applied between 7.5 and 8 Å radial distance.⁷

Every fiftieth configuration is used in the subsequent spectral evaluation, a total of 600 configurations. For the present work, we compute all electron-water interactions without cutoff in the minimum-image convention, using the configurations generated from the path-integral simulation. The additional interaction range produces an additional binding energy for the electronic states of approximately 0.9 eV, compared with that evaluated with the spherical cutoff, displacing the density of states essentially uniformly. However, no statistically significant effect on the calculated absorption spectrum is observed. Neglect of even longer-range interactions restricts our ability to calculate absolute energies precisely, with a small additional binding energy being expected in an infinite solvent sample.

The one-electron eigenstates are obtained very efficiently with a regularly spaced three-dimensional grid for numerical representation in real space and a split-Fourier propagation^{8,9} in imaginary time to project the ground state from a trial function.⁹ Excited states are obtained by the same procedure after orthogonalization to all lower energy eigenstates. We evaluate the ground and the first nine excited states for each of the 600 solvent configurations. All states are evaluated with use of a numerical grid of 16 points per dimension within a cube of edge length 12.33 Å, centered at the electronic

center of mass of the electron path from the path-integral simulation. Doubling both values produces no statistically significant changes from the results presented below.

The equilibrium structural characterization of the simulated system has been reported previously.³ For the purpose of the present investigation, we emphasize only that the excess electron creates a polaron-type state, with the excess electron occupying a cavity in the polarized solvent.

The density of states obtained is shown in Fig. 1. Three kinds of states can be clearly distinguished as indicated in the figure. The ground state (E_0) is always a bound state as expected for an excess electron in a polar fluid.¹ Its energy distribution is centered around -3.4 eV which is the sum of -5.7 eV potential energy and $+2.3$ eV quantum kinetic energy. The extreme values found -4.8 and -2.4 eV, illustrate that the fluctuation amplitude is clearly large, exceeding thermal energies (0.025 eV) by more than 1 order of magnitude. This is not surprising if it is recalled that the binding energy of a single molecule in pure liquid water fluctuates comparably.¹⁰

A typical ground-state wave function is shown in the upper left-hand panel of Fig. 2; it displays qualitatively the symmetry properties of an s -type state. The mean ground-state radii, defined by

$$\langle r_A \rangle \equiv \left\langle \int \rho(\mathbf{r}) |\mathbf{r}| d\mathbf{r} \right\rangle \quad (1)$$

or

$$\langle r_B \rangle \equiv \left\langle \int \rho(\mathbf{r}) r^2 d\mathbf{r} \right\rangle^{1/2}, \quad (2)$$

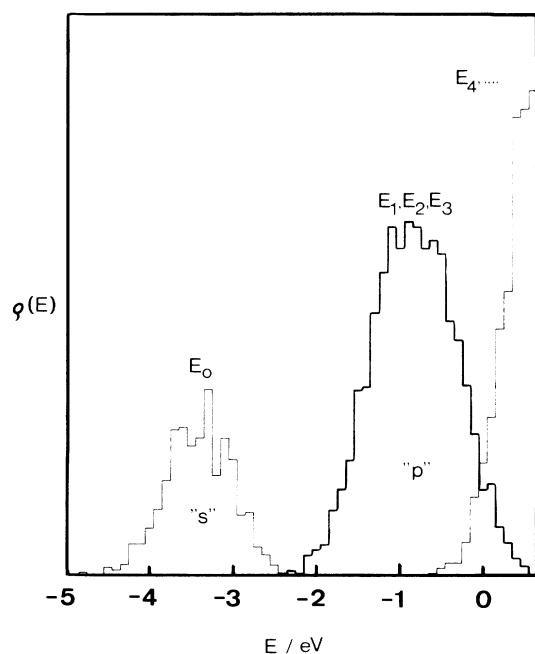


FIG. 1. Density of electronic states.

yield 1.9 and 2.1 Å, respectively. A difference between the two radii is observed in any given configuration: $\langle r_B - r_A \rangle = 0.2$ Å, and, hence, the ground-state wave functions are relatively broadened in comparison with ideal Gaussian wave packets.

The mean square fluctuation of the ground-state radius is only about 0.1 Å, with use of either of the two definitions given above, relatively small compared with that conjectured, e.g., for the case of excess electrons in liquid ammonia.¹¹

Returning to Fig. 1, it is clear that the density of states for the lowest three excited states (E_1 , E_2 , and E_3) is similar in appearance to that for the ground state. The wave functions corresponding to this three-state manifold are always found to be localized with a radius of about 3 Å; contour plots for a typical configuration are shown in Fig. 2. It is obvious that these orbitals are p -like with one node and with approximately mutually perpendicular orientations.

The energetic distribution of the p -like states extends between -2.4 and $+0.8$ eV, and thus only the energetically highest of these states, and this only occasionally, is unbound. Most importantly, this triple of localized states is distinctly nondegenerate: The most probable energy splitting between the lowest (E_1) and highest (E_3) eigenvalue is about 0.8 eV, and in 95% of the configurations, this splitting exceeds 0.4 eV. This removal of degeneracy reflects typically distorted solvent cavities. Although the significance of this phenomenon has been pointed out, the importance of this feature, manifest here, is at odds with previous estimates based on simplified models.¹²

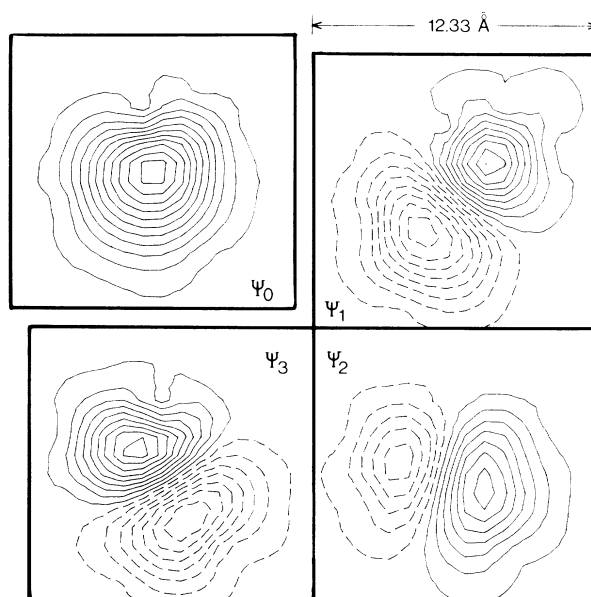


FIG. 2. Electronic wave-function contour plots for typical ground state and lowest three excited states.

Finally, for the fourth and all higher excited states (E_4, \dots) a monotonically increasing density of states is found that is analogous to the pattern for a free-electron gas. The distributions shown is truncated at an energy of +0.6 eV which is the lowest energy found for the highest (ninth) excited state calculated here. The fourth and higher excited states are in fact delocalized in the sense that the electronic amplitude does not decay significantly over the range of the computational grid. For the limiting case of free states in an infinitely large box, an energetic continuum is expected.

In principle, the lower edge of the conduction band can be inferred from Fig. 1. With the occasional exception of the fourth excited state, all "continuum" states lie at positive energies. Accordingly, the band edge can be located at a vanishing or just slightly negative energy.

We now turn to the absorption spectrum. The optical spectrum corresponding to unpolarized incident light is displayed in Fig. 3. We show the line shape obtained up to an energy of 4.1 eV, which corresponds, as above, to the lowest energy found for a transition into the highest calculated (ninth) excited state. The total oscillator strength we obtain is about 94% (or 92% if we only include the transitions up to $\Delta E = 4.1$ eV as in Fig. 3) of that required by the Thomas-Reiche-Kuhn sum rule, and consists of 31%, 30%, 28%, and 5% for transitions into the first, second, and third p -states and into the higher-energy delocalized states, respectively. An exhaustive treatment of the higher excited states would yield the complete oscillator strength. From the experimental absorption band, an oscillator strength of about 0.75

has been deduced, with an uncertainty as high as 20%–30%.¹³ An additional band in the uv region has been reported, but appears to be due to perturbed electronic transitions of the solvent.¹⁴ Therefore, the agreement between experiment and the calculated *one-electron* model oscillator strength is satisfactory.

The calculated spectrum has its absorption maximum at an energy of about 2.4 eV and a half width of about 1.1 eV; the experimental figures are 1.7 and 0.8 eV, respectively.¹³ The overestimate of the band maximum is in line with previous path-integral estimates for both the hydrated^{3,15} and ammoniated¹⁶ electron. This discrepancy is likely due to inadequacies of the model electron-water pseudopotential.² The pseudopotential of Wallqvist, Thirumalai, and Berne¹⁷ yields an estimated average excitation energy closer to the experimental value, although a corresponding band shape remains to be determined. We emphasize in this context that we describe the simulated system without any attempt to adjust parameters to produce quantitative agreement with experiment. It is therefore particularly noteworthy that the half width of the absorption spectrum is slightly *overestimated* by our calculation, in contrast to earlier more empirical models.¹

The present simulation approach allows the assignment of the physical origin of this large half width. First, the solvent cavities fluctuate in radial size and thus cause a variation of the excitation energies as expected from a simple particle-in-a-box model. Second, the cavities are nonspherical, so that excitations into the p -type states are typically significantly nondegenerate. In the inset of Fig. 3 we show the decomposition of the separate subbands for the s - p transitions. The energy splitting is typically 0.4 eV for adjacent s - p transitions and accordingly about 0.8 eV between the lowest (ΔE_{10}) and highest (ΔE_{30}) s - p transition.

The contributions to the width from radial fluctuations and cavity distortions are comparable in our simulation. That is, only about half of the total half width is obtained from a spectrum obtained by averaging over the s - p transitions: $\Delta E = (\Delta E_{10} + \Delta E_{20} + \Delta E_{30})/3$. In general, it appears that the significance of asymmetry has been underestimated in simpler models, even in those which emphasize heterogeneous broadening.¹⁸

Of course the extent of nondegeneracy fluctuates with fluctuations in the solvent cavity asymmetry, including contributions from both position and orientation of the solvent. If the ground-state electronic distribution (which reflects the full potential surface) is translated into the geometry of an ideal rotational ellipsoid, the difference between the lengths of the smallest and largest principal axes is on the average about 8%, and the distribution of this difference is centered at a nonzero value. The deviation from a symmetric distribution is therefore relatively small. Nevertheless, since the number of distorted configurations (i.e., those with two unequal principal axes) must greatly exceed the number of symmetric

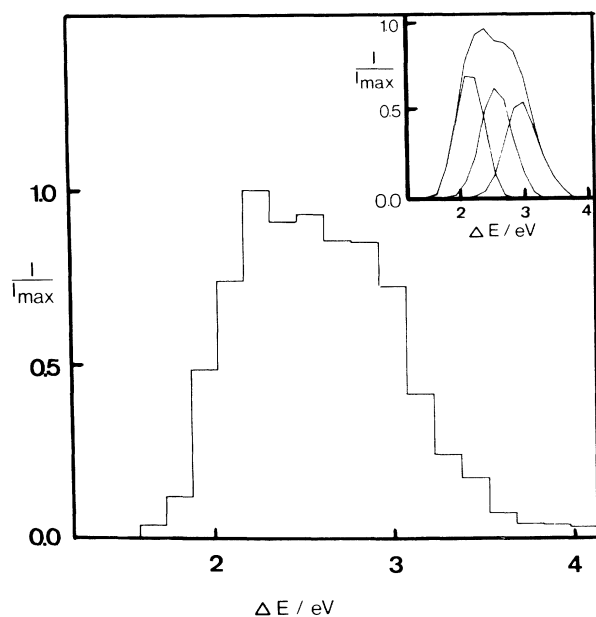


FIG. 3. Simulated optical absorption spectrum of an excess electron in liquid water. Inset: Decomposition into separate subbands for the three s - p transitions.

configurations, the most probable result at finite temperature is that of a somewhat asymmetric potential surface. What is perhaps surprising, and not simply predictable, is the relatively large size of the splitting in the p -type energy levels. However, the observed result is only about twice as large as that expected for the simplest possible model, that of a particle in a box with corresponding asymmetry in the side lengths.

We have no reason to believe that the importance of asymmetry found here is peculiar to water or even polar liquids. The arguments favoring asymmetry are generic to fluids, although the quantitative correlation between energy splitting and asymmetry is likely to be fluid dependent (the particle in a box being one extreme caricature). Solvated-electron spectra, in fact, exhibit substantial variation in their quantitative characterization from one medium to another. The expectations expressed here must, of course, be tested by further studies of the type described in the present article for a variety of liquid media.

Another important but poorly understood feature of the hydrated-electron spectrum is its pronounced asymmetry. Figure 3 demonstrates that our simulated spectrum is indeed asymmetric, although the high-energy tail is not fully developed. Some asymmetry is obtained from consideration of only the s - p transitions as can be seen from the inset of Fig. 3. Of at least equal importance, however, are the transitions into energetically higher, delocalized states. As described above, the contribution of these bound-continuum transitions to the total oscillator strength is about 10%.

Two questions not addressed by our model calculation are the significance of vibronic coupling with the solvent modes and of nonlocal excess-electronic transitions between different potential wells. Both have been conjectured¹⁹ as contributing to the line shape. We refrain from adding to the already abundant speculations about these phenomena here. The role of such effects in providing quantitative agreement between theory and experiment remains to be determined. We note that the issue of motional narrowing does not arise within the present calculation, since the computed spectrum is the envelope of a distribution of δ -function peaks, and the full width is so large as to rule out a contribution from averaging over solvent motions.

In summary, we have calculated the optical-absorption spectrum of the hydrated electron directly from the quantum statistical mechanics of a Hamiltonian based on elementary principles. Its physical nature is then subject to direct and detailed analysis. Our calculations show that the dominant spectral excitations in the equilibrium hydrated state are to bound localized p -type states, with a high-energy tail comprised of excitations into an unbound, apparently delocalized continuum. The large spectral half width follows from comparable contributions due to radial fluctuations of the solvent cavities and their ubiquitously distorted shapes. In consideration

of the similarity of solvated-electron spectra in many polar liquids, it is likely that our conclusions also apply to the spectra of excess electrons in these other disordered media.

This work was supported by the National Science Foundation (Materials Research Group, DMR8418086) and by grants from the Robert A. Welch Foundation to two of us (P.J.R. and R.A.F.), who are also recipients of Dreyfus Foundation Teacher-Scholar Awards. One of us (R.A.F.) is an Alfred P. Sloan Foundation Fellow. Another of us (P.J.R.) is the recipient of a National Science Foundation Presidential Young Investigator Award and a National Institutes of Health Research Career Development Award from the National Cancer Institute, U.S. Department of Health and Human Services.

¹D.-F. Feng and L. Kevan, *Chem. Rev.* **80**, 1 (1980); N. R. Kestner, in *Electron-Solvent and Anion-Solvent Interactions*, edited by L. Kevan and B. Webster (Elsevier, Amsterdam, 1976).

²J. Schnitker and P. J. Rossky, *J. Chem. Phys.* **86**, 3462 (1987).

³J. Schnitker and P. J. Rossky, *J. Chem. Phys.* **86**, 3471 (1987).

⁴H. J. C. Berendsen, J. P. M. Postma, W. F. Van Gunsteren, and J. Hermans, in *Intermolecular Forces*, edited by B. Pullman (Reidel, Dordrecht, 1981).

^{5a}R. F. Feynman, *Statistical Mechanics* (Benjamin, Reading, 1972).

^{5b}D. Chandler and P. J. Wolynes, *J. Chem. Phys.* **74**, 4078 (1981).

⁶H. C. Andersen, *J. Chem. Phys.* **45**, 335 (1982).

⁷O. Steinhauser, *Mol. Phys.* **45**, 335 (1982).

⁸M. D. Feit, J. A. Fleck, Jr., and A. Steiger, *J. Comput. Phys.* **47**, 412 (1982).

⁹R. Kosloff and H. Tal-Ezer, *Chem. Phys. Lett.* **127**, 223 (1986).

¹⁰F. Hirata and P. J. Rossky, *J. Chem. Phys.* **74**, 6867 (1981).

¹¹P. F. Rusch, W. H. Koehler, and J. J. Lagowski, in *Metal-Ammonia Solutions*, edited by J. J. Lagowski and M. J. Sienko (Butterworths, London, 1970).

¹²N. R. Kestner and J. Logan, *J. Phys. Chem.* **79**, 2815 (1975).

¹³F.-Y. Jou and G. R. Freeman, *J. Phys. Chem.* **83**, 2383 (1979).

¹⁴S. O. Nielsen, B. D. Michael, and E. J. Hart, *J. Phys. Chem.* **80**, 2482 (1976).

¹⁵M. Sprik, R. W. Impey, and M. L. Klein, *J. Stat. Phys.* **43**, 967 (1986).

¹⁶M. Sprik, R. W. Impey, and M. L. Klein, *J. Chem. Phys.* **83**, 5802 (1985).

¹⁷A. Wallqvist, D. Thirumalai, and B. J. Berne, *J. Chem. Phys.* **86**, 6404 (1987).

¹⁸W. M. Bartczak, M. Hilczer, and J. Kroh, *J. Phys. Chem.* **91**, 3834 (1987).

¹⁹A. Banerjee and J. Simons, *J. Chem. Phys.* **68**, 415 (1978); G. A. Bogdanchikov, A. I. Burshtein, and A. A. Zharikov, *Chem. Phys.* **107**, 75 (1986).